

UCLA

UCLA Previously Published Works

Title

Kevlar/vinyl ester composites with SiC nanoparticles

Permalink

<https://escholarship.org/uc/item/5m02c2f1>

Journal

SAMPE Conference Proceedings, 49(2004)

Authors

Yong, Virginia

Hahn, H. Thomas

Publication Date

2004-05-20

Peer reviewed

KEVLAR/VINYL ESTER COMPOSITES WITH SiC NANOPARTICLES

Virginia Yong¹ and H. Thomas Hahn^{1,2}

¹Materials Science & Engineering Department

²Mechanical & Aerospace Engineering Department
UCLA, Los Angeles, CA 90095

ABSTRACT

Kevlar/vinyl ester composites with SiC nanoparticles were fabricated using hand lay-up. Vacuum and mechanical press were used to suppress porosity, increase the fiber volume fraction and assist infiltration. The SiC nanoparticles were examined using TEM and TGA, and were vacuum-baked at 200°C to remove adsorbed moisture, as per TGA measurement. *Gamma*-methacryloxy propyl trimethoxy silane (MPS) was chosen as the coupling agent and its dosage was calculated to achieve monolayer coverage. Both mixing routes with (1) the nanoparticles pretreated with a dilute MPS solution in an acid 5% (v/v) water-ethanol mixture and (2) the MPS sonicated as an integral blend with the filled vinyl ester, were attempted. FTIR was used to study the silanol condensation between MPS and the SiC nanoparticles. X-ray inspection and x-sectioning were performed on the nanocomposite panels. The modulus from 3-point bend tests showed an increase for both mixing routes, whereas strength increased for route (2) but decreased for route (1). The increases in modulus and strength are likely attributed to the better dispersion quality as observed under the optical microscope and AFM, lower resin viscosity, lower porosity, and a stronger coupling/bonding between the SiC nanoparticles and vinyl ester resin as a result of the MPS addition. The decrease in strength in route (1) was likely caused by the siloxane layer between the SiC nanoparticles associated with the three reactive silanols per molecule of MPS. A 19% increase in tensile strength was found in route (2) with 1 vol. % SiC addition, which confirmed the high potential of nanoparticles in enhancing the mechanical properties of structural composites.

KEY WORDS: Aramid Fiber, Esters/Vinyl Esters, Nanocomposites

1. INTRODUCTION

It is expected that the next generation of high-performance structural materials will routinely employ nanoparticles and nanocomposites. The unique properties of nanoparticles arise from their size reduction. When a particle is reduced down to the nanosize range (usually defined as

1-100nm), a much larger surface-to-volume ratio is achieved, and consequently, a nanocomposite may exhibit special properties arising from phase interactions at interfaces [1].

Kevlar aramid [PPTA; poly(*p*-phenylene terephthalamide)] fiber is widely used in manufacture of advanced composites because of its high tensile modulus, strength, toughness, and thermal stability. The low viscosity coupled with rapid curing rate at room temperature and relatively low cost of vinyl ester resins have led to their extensive use as matrix materials for reinforced composites. Covalent ceramic materials like silicon carbide (SiC) have been recognized as potential candidates for structural applications because of their superior mechanical properties (strength, stiffness and hardness), chemical (oxidation and corrosion resistance) and thermal stability at high temperatures. This paper investigates the feasibility of improving Kevlar/vinyl ester composites using 30-nm SiC nanoparticles.

2. EXPERIMENT

2.1 SiC Nanoparticles Characterization

Transmission electron microscopy (TEM) was used to characterize the size distribution of SiC nanoparticles. TEM sample preparation was carried out by diluting the SiC nanoparticles with isopropyl alcohol (IPA) and sonicating the suspension at 40W for 10mins. A drop of the sonicated suspension was then put on the Prod #01800 Ted Pella 200 mesh specimen support film grids. Only SiC nanoparticles were left for TEM examination on the support film after the evaporation of IPA solution.

As-received SiC nanoparticles were heated both in air and in nitrogen to 1000⁰C using a thermogravimetric analysis (TGA) to examine the moisture adsorption on the SiC surface. Weight changes of the specimen were recorded at 10⁰C/min.

2.2 Nanocomposite Processing and Characterization

A nonionic methacrylate ester-functional silane, *gamma*-methacryloxy propyl trimethoxy silane (MPS), was chosen as the coupling agent and dispersant. The organofunctional group “methacrylates” exhibits the best wet strength with polyester and the functional group – (CH₂)₃Si(OMe)₃ of methacrylate additive exhibits the highest flexural strength of polyester glass laminates [2]. The amount of MPS dosage was calculated to be 67 wt. % of SiC to achieve monolayer coverage.

Both mixing routes of MPS pretreated SiC nanoparticles and in situ addition were attempted. MPS was applied directly to the particles by treating the SiC nanoparticles for several minutes with a dilute MPS solution in an acetic acid 5% (v/v, to achieve pH of 2-4) water-ethanol mixture [2, 3]. RSi(OH)₃ has maximum stability at pH 2-4 and it is more effective on acidic oxide surfaces than on basic oxide surfaces. The surface was then rinsed with ethanol and dried at ~100⁰C in vacuum for 24 hrs to remove water and promote the reaction between SiC nanoparticles and adsorbed silane. FT-IR was used to study the silanol condensation between

MPS and the SiC nanoparticles. The result is usually a multilayer coating (3-10 layers). The functional group $-(\text{CH}_2)_3\text{Si}(\text{OMe})_3$ reacts with hydroxylated SiC surfaces through hydrogen bonding and through covalent siloxane (Si-O-Si) bonds as shown in Figure 1. In addition, the organofunctional group “methacrylates” could copolymerize with styrene monomers in the vinyl ester during cure [4]. Therefore, MPS may act as a bridge to bond the SiC to the vinyl ester resin with a chain of covalent bonds. This could lead to the strongest interfacial bond.

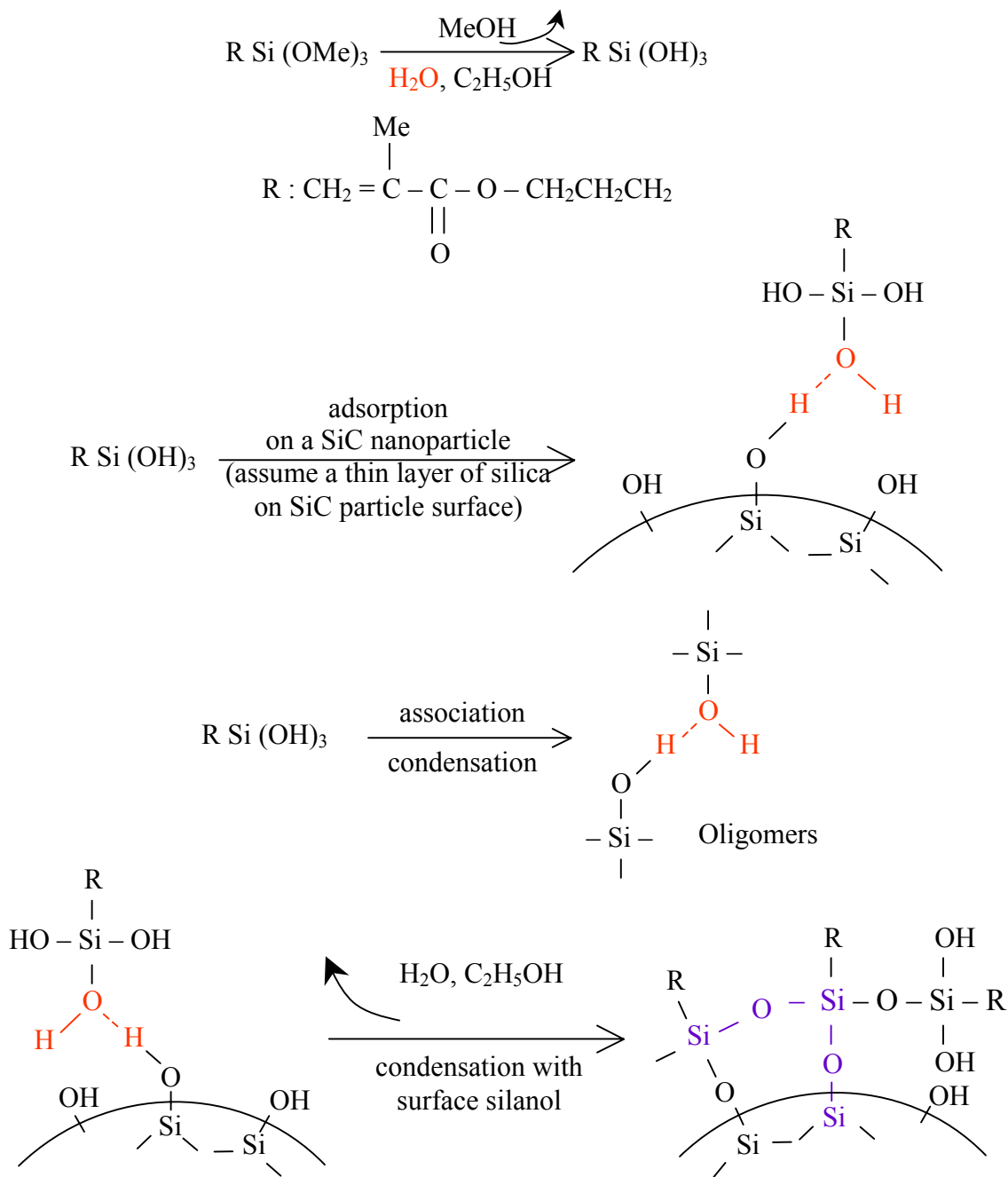


FIGURE 1 Deposition of MPS on a SiC particle. MPS oligomers adsorb on the particle and condense with surface silanol aided by a distillation of ethanol.

Since the energy of wetting must exceed the interparticle binding energy and the process is liquid diffusion limited, mechanical force is required (we used ultrasonic disperser and magnetic stirrer) to separate the agglomerates of particles and permit the MPS to adsorb onto the unwet portions of the SiC surface. SiC (with an average diameter of 30-nm)/vinyl ester nanocomposites were mixed under the following conditions:

- Resin (Derakane momentum 411-350) volume: 150 ml
- Sonication (24W) + magnetic stirring (cooled with compressed air): 1.5 hr
- Degassing in vacuum for 1.5 hr
- Trigonox (catalyst): 2.0 wt.%
- CoNap (promoter): 0.3 wt.%
- Post-cure at 85⁰C for 1 hr

Nanoparticles dispersion was characterized by both the optical microscopy and the AFM in force modulation (contact mode) and in phase imaging (tapping mode). The different stiffnesses of the SiC and vinyl ester resin matrix are manifested by the two different signals with a phase difference, and SiC particles (stiffer component) were seen as locations with brighter contrast.

2.3 Fiber Composite Fabrication and Characterization

Kevlar/vinyl ester composites were fabricated using hand lay-up. Theoretical maximum fiber volume fraction was calculated based on the Kevlar 29 fabric thickness measured under atmospheric pressure compression using autoclave, which was determined to be 61%. Calculation was as follows:

At 29.6 In Hg: -

Thickness of one ply = 0.504 mm

% strain under compression = 12.4 %

Fiber volume: -

$$V_k = W_k / \rho_k = 35.645 / 1.440 = 24.753 \text{ cm}^3$$

Total volume: -

$$V = L.W.t = 5 \text{ in} \times 5 \text{ in} \times 0.504 \text{ mm} \times 5 \text{ plies} = 40.645 \text{ cm}^3$$

Resin volume: -

$$V_r = V - V_k = L.W.t - W_k / \rho_k = 40.645 - 24.753 = 15.892 \text{ cm}^3$$

Therefore, theoretical maximum fiber volume fraction using Kevlar 29 under atmospheric pressure compression was calculated to be $V_k / V = 24.753 / 40.645 \times 100\% = 61\%$.

A mechanical press in conjunction with vacuum was used to increase the fiber volume fraction, suppress voids, and assist infiltration. A zero-bleed net resin system was employed to reduce porosity [5]. Bleeder was eliminated so as to prevent pressure gradient drop associated with bleeding at the bleeder ply. A well-fitted dam was used to prevent pressure drop at the laminate boundary associated with free bleeding.

3. RESULTS AND DISCUSSION

3.1 Characterization and Pre-treatment of SiC Nanoparticles

Figure 2 shows TEM micrographs at 100kX and 250kX, which indicate a good size distribution of SiC nanoparticles with an average diameter of around 30nm, as specified by the manufacturer.

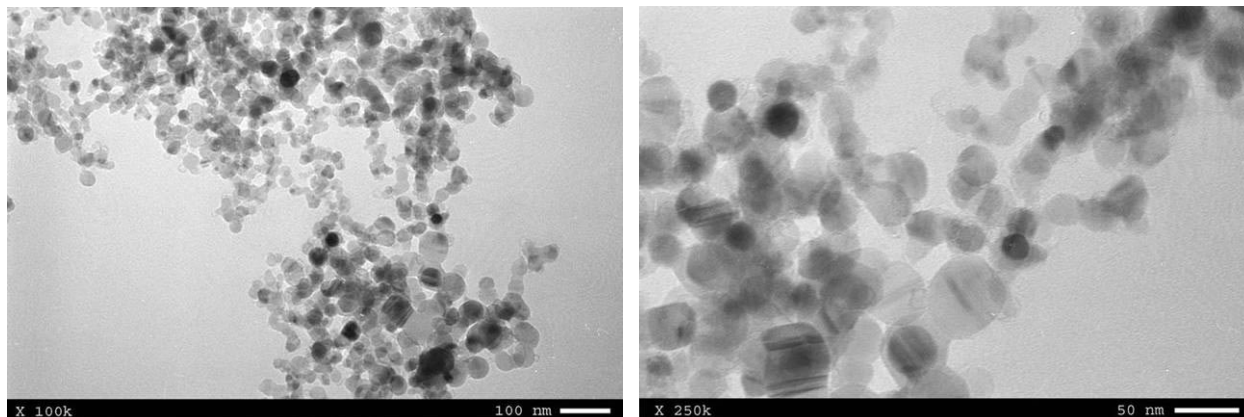
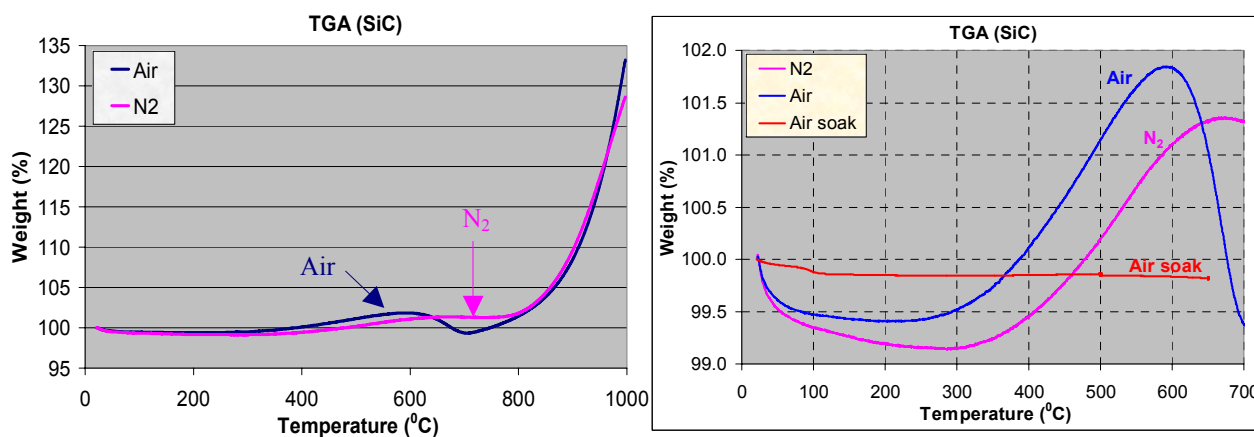


FIGURE 2 TEM micrographs of SiC nanoparticles at 100kX and 250kX.

TGA at a heating rate of $10^{\circ}\text{C}/\text{min}$ shows a maximum weight loss at 200°C as shown in Figure 3, which was assigned to the loss of water. This water derived partially from endothermic condensation of Si-OH groups and partially from evolution of free water which was adsorbed due to the hydrophilic SiC surface [2, 6]. Water increases one particle surface's affinity for another, which excludes organic molecules within agglomerates. Also, water is difficult to remove from particle surfaces once these are immersed in organic liquids as illustrated by the considerably higher heat of wetting by water compared to organic liquids [7]. Therefore all SiC nanoparticles were pre-treated by vacuum baking at 200°C for 24 hrs to remove the adsorbed moisture. A minor oxidation started at approximately 260°C followed by the main oxidation process beginning at approximately 750°C [8], which resulted in the weight increase. The weight loss began at approximately 600°C in air is attributed to the oxidation of carbon [9].



(A) TGA of as-received SiC nanoparticles

(B) Enlarged view at temperature range from 0 to 700°C

FIGURE 3 TGA shows a maximum weight loss at 200°C .

3.2 Nanocomposite Processing and Characterization

FT-IR was performed to study the silanol condensation between MPS and the SiC nanoparticles. KBr discs were used, prepared by compressing a finely ground mixture of 0.75 mg of the sample and 200 mg of infrared grade KBr powder. Figure 4 shows FT-IR spectra over the range of 4500 to 400 cm^{-1} . Curve 1 is the IR spectrum of as-received SiC nanoparticles before vacuum baking pre-treatment at 200 $^{\circ}\text{C}$. An intense absorption band at $\sim 800 \text{ cm}^{-1}$ (the TO phonons) with a shoulder at 912.5 cm^{-1} was observed, which is attributed to the Si-C stretching vibration mode in crystalline cubic β -SiC [10]. The band at 2340 cm^{-1} was assigned to CO_2 gas. A small intensity and broad absorption band in the range from 3550 to 3300 cm^{-1} could be due to the silanol groups Si-OH and the band broadening was assigned to hydrogen bonding between distinct groups of hydroxyls [11], which indicates that the as-received SiC surface was partially oxidized. Curve 2 and 3 show MPS pretreated SiC nanoparticles before and after $\sim 100^{\circ}\text{C}$ drying respectively. The bands corresponding to the C-H_n bending mode and Si-OH group at 900 cm^{-1} were superimposed on the shoulder of the 912.5 cm^{-1} SiC absorption. Also, The broad absorption band at 1200-1000 cm^{-1} was due to the overlapping of the band due to CH_2 bending in Si-(CH₂)_n-Si at 1020 cm^{-1} , the bands due to methoxy group OCH₃ (1193, 1090 cm^{-1}), C-O stretching (1200 cm^{-1}), and a broad band due to Si-O stretching in Si-O-Si and Si-O-C (from 1130 to 1000 cm^{-1}). C-H_n bending (1450-1350 cm^{-1}), O-H bending (1640 cm^{-1}), C=C stretching (1670 cm^{-1}), and C=O stretching (1720 cm^{-1}) could have contributed to the broad band from 1700 to 1300 cm^{-1} [12]. The band at 2950-2900 cm^{-1} was assigned to C-H_n stretching. The intensity of O-H stretching band in Si-OH at 3380 cm^{-1} decreased after drying, which could have been contributed by the silanol condensation between MPS and the SiC nanoparticles.

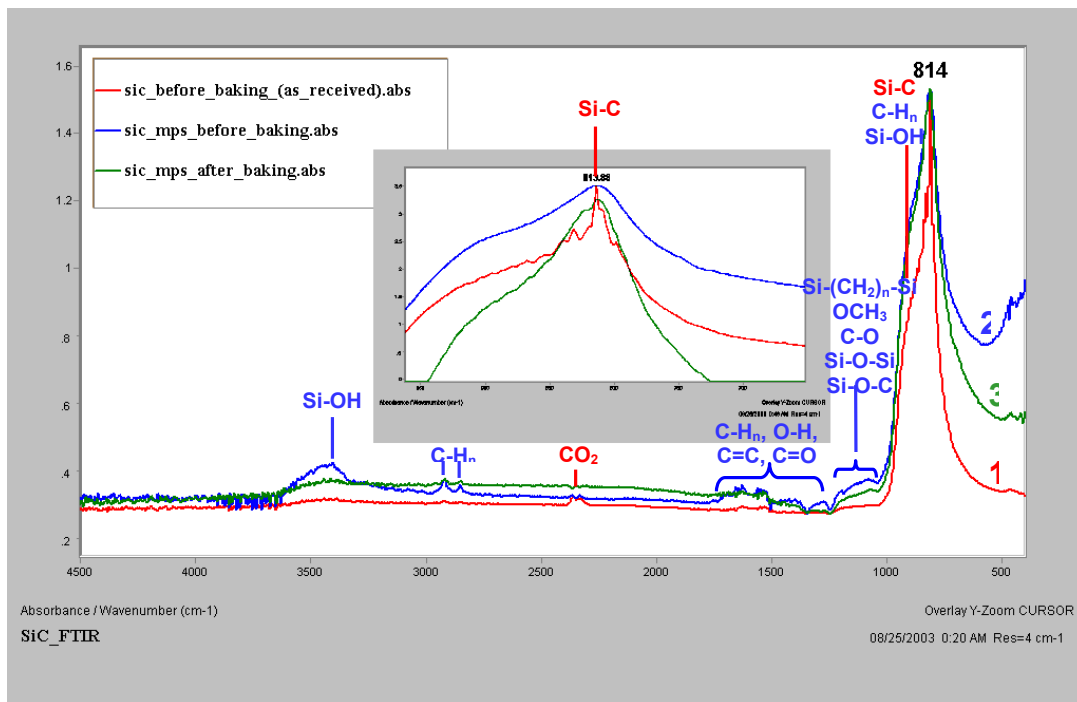


FIGURE 4 FT-IR spectra of SiC samples. (1) as-received SiC nanoparticles; (2) and (3) MPS pretreated SiC nanoparticles before and after $\sim 100^{\circ}\text{C}$ drying respectively. Inset: an enlarged view of a strong characteristic absorption peak at $\sim 800 \text{ cm}^{-1}$, which is attributed to the transverse-optical phonons of Si-C bonds in 3C-SiC.

Optical photographs of Figure 5 show the state of dispersion of untreated-SiC particles in vinyl ester resin after sonication. As resolution of optical microscopy limited by the wavelength of visible light is around 0.5- μm at a magnification of 2kX, optical photographs at 100X confirmed the agglomerated SiC nanoparticles at micron scale. The optical inspection indicates that a homogeneous mixture (to a certain extent) was obtained by sonication, however ultrasonic agitation could not break up all of the agglomerates [13].

Optical photograph at 100X

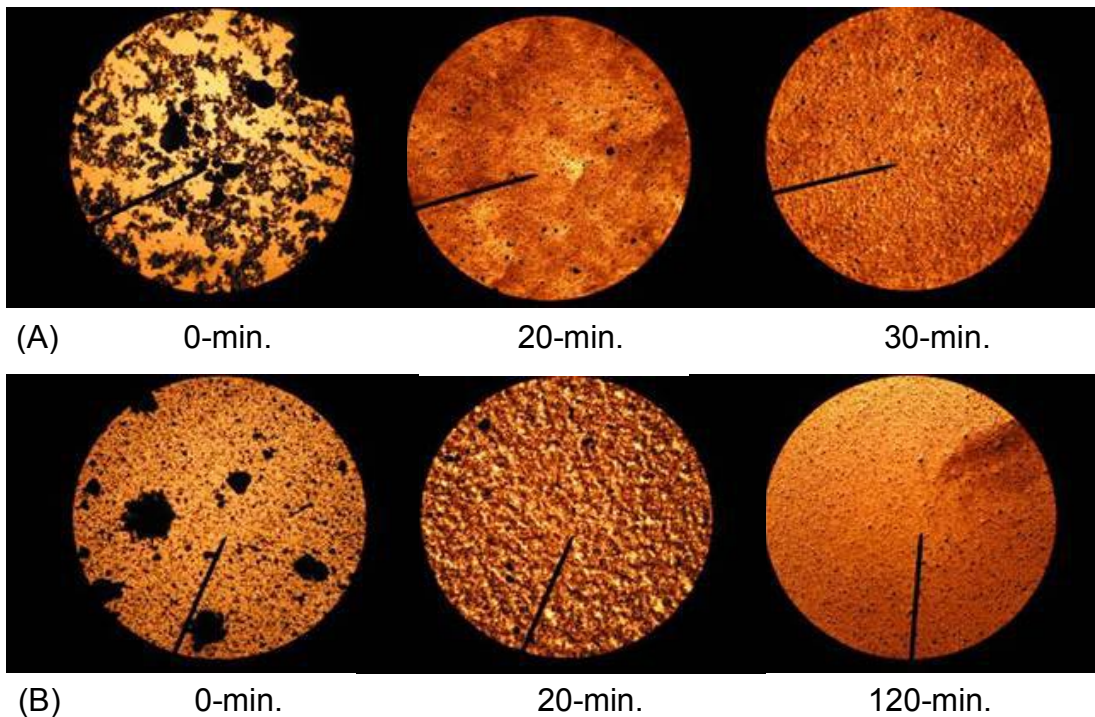
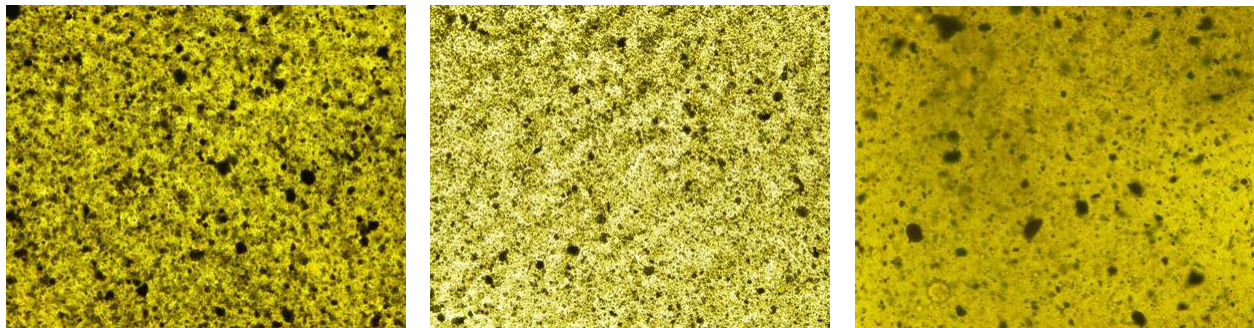


FIGURE 5 Dispersion quality of sonicated-dispersed SiC/vinylester samples with different sonication time (A) 1 vol. % - 20 ml; (B) 1 vol. % - 120 ml

Figure 6 shows the optical photographs at 100X of 1 vol. % SiC samples. In situ mixing labeled as S/N 2 was found to have a better dispersion.



S/N 1: Without dispersant S/N 2: MPS – In situ mixing S/N 3: MPS – SiC pretreat

FIGURE 6 Optical photographs at 100X of 1 vol. % SiC samples

Particle dispersion characterization via AFM confirmed the better dispersion for MPS in situ mixing (S/N 2) as compared to without MPS (S/N 1) and MPS pretreated SiC nanoparticles (S/N 3). An average agglomerated particle size of 0.647- μm , 0.351- μm , and 1.251- μm were found for S/N 1, 2, and 3 respectively. Figure 7 shows the AFM images in phase imaging (tapping mode) and in force modulation (contact mode) for the MPS in situ mixing specimen.

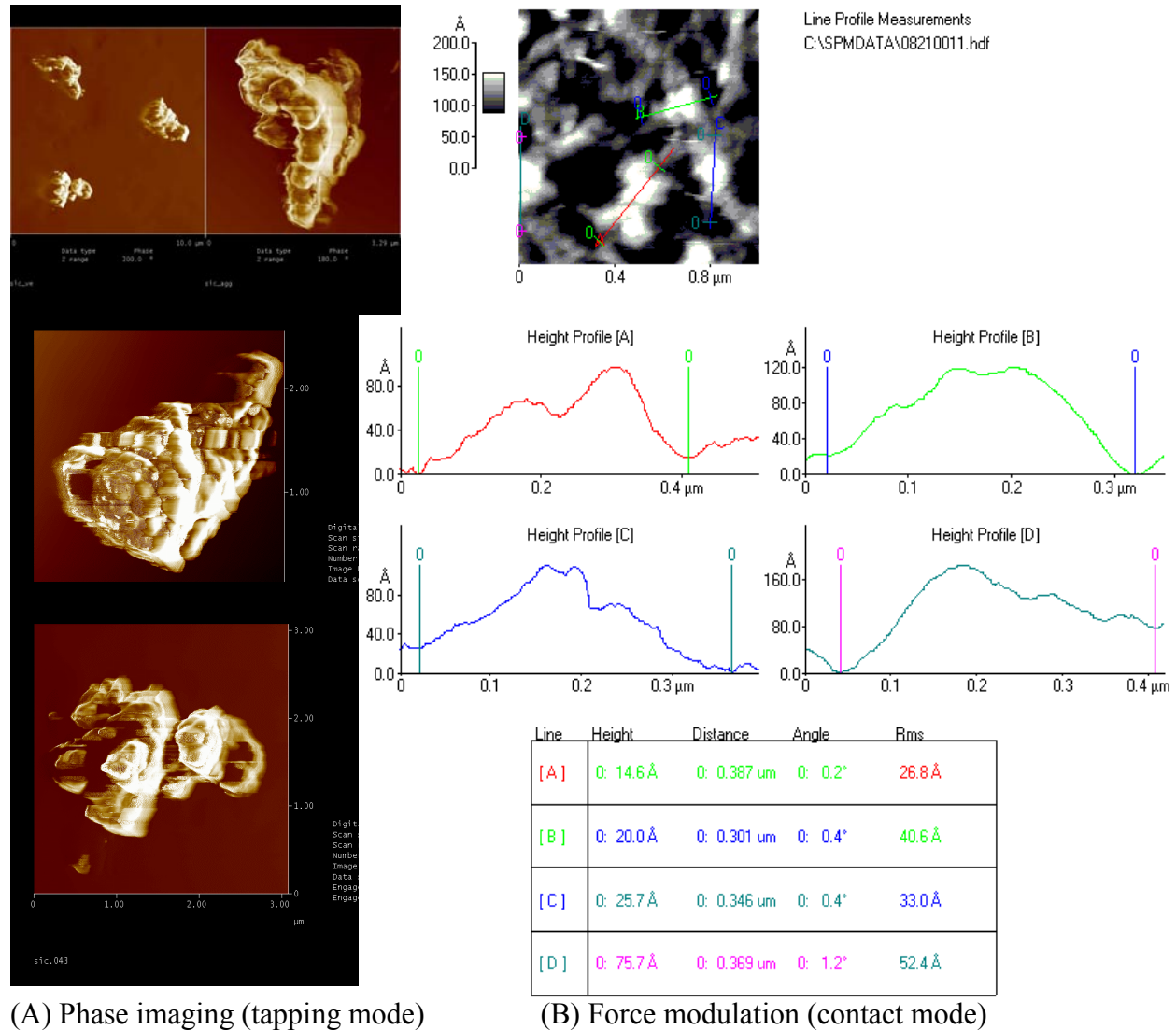


FIGURE 7 AFM for SiC/vinyl ester dispersion characterization.

3-point bending tests were carried out per ASTM D790 “Standard Test Methods for Flexural Properties of Unreinforced and Reinforced Plastics and Electrical Insulating Materials” using Procedure A. The modulus from 3-point bend tests shows an increase with or without MPS, whereas strength increases for MPS in situ mixing but decreases for both MPS pretreated SiC and mixing without MPS, Figure 8. The increase in strength for MPS in situ mixing is likely attributable to the better dispersion quality as observed under the optical microscope and AFM (Figure 6 and 7), lower porosity [2], and a stronger interfacial bonding between the SiC nanoparticles and vinyl ester resin as a result of the MPS addition. The decrease in strength for

MPS pretreated SiC nanoparticles is likely caused by the siloxane layer between the SiC nanoparticles associated with the three reactive silanols per MPS molecule.

SiC vol. %	Mixing condition	Ultimate flexural stress σ_{max} (MPa)		Flexural modulus E (GPa)	
		Mean	S.D.	Mean	S.D.
0	Neat resin	116	16	2.9	0.11
1	Without dispersant	63	4	3.6	0.07
2		53	1	3.7	0.07
1	MPS - In situ	126	11	3.5	0.28
	MPS - SiC pretreat	77	22	3.5	0.19

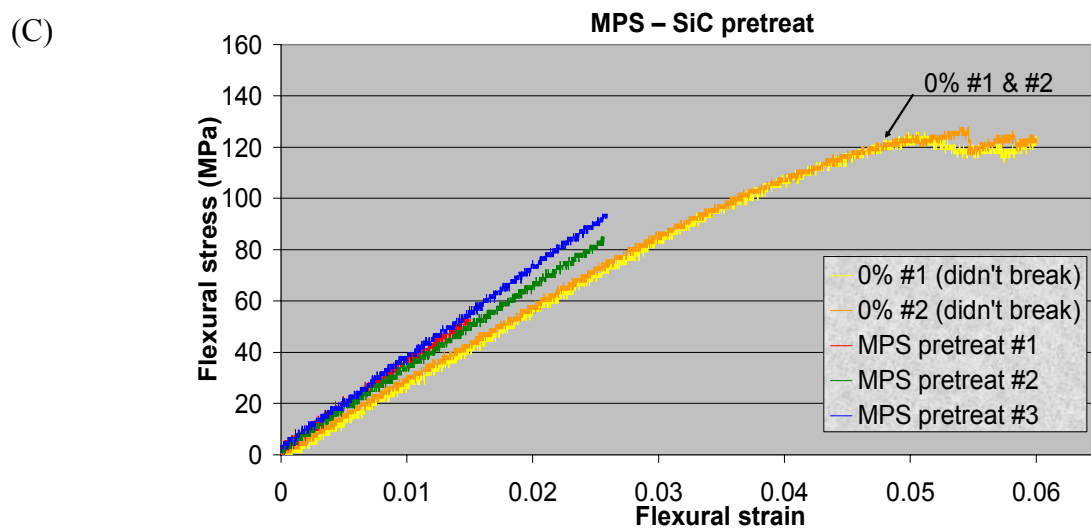
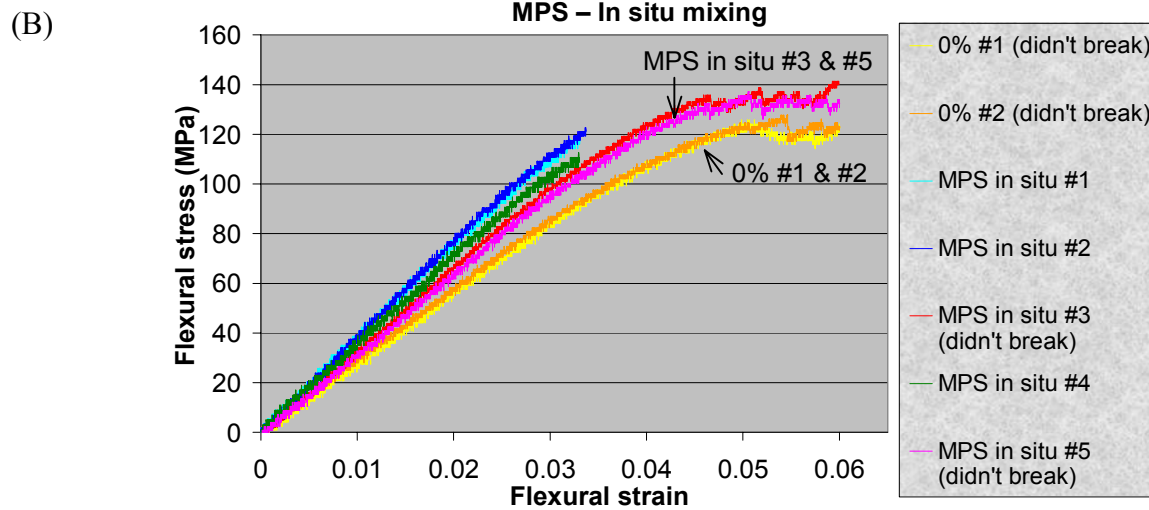
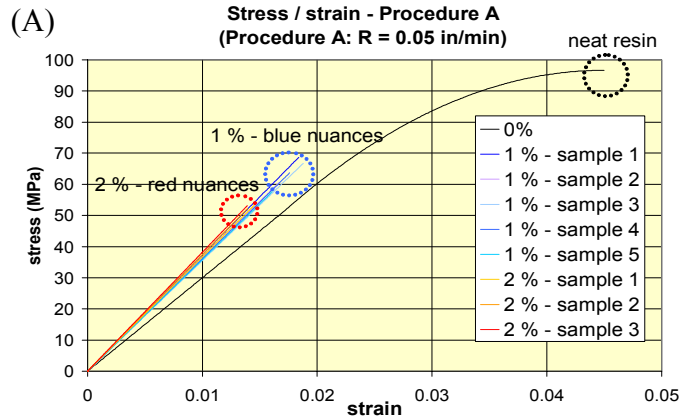


FIGURE 8 Stress vs. strain curve of (A) 0, 1, 2 vol. % SiC without dispersant; (B) and (C) 0%, 1 vol. % SiC with MPS via in situ addition and pretreated SiC respectively.

3.3 Fiber Composite Fabrication and Characterization

X-ray inspection and cross-sectioning were performed on the 1 vol. % SiC Kevlar/vinyl ester composite panels. Resolution of the x-ray is not good enough to observe the nanoparticle dispersion. Agglomerates of SiC particles are seen in the interface regions between Kevlar layers, Figure 9. This may be the result of filtering of particles during resin impregnation. Nevertheless, smaller SiC particles are found inside Kevlar layers as well.

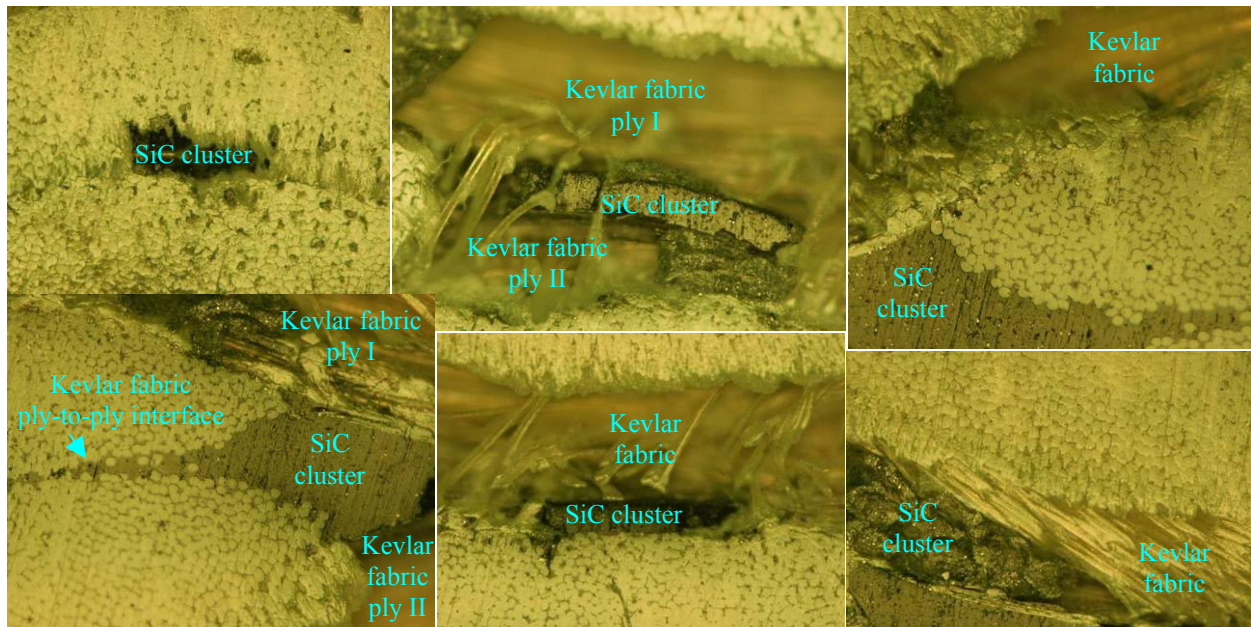


FIGURE 9 Optical photographs at 100X of polished x-sectioned 1 vol. % SiC Kevlar/vinyl ester composite panel specimen.

Tensile tests were carried out per ASTM D3039/D3039M “Standard Test Method for Tensile Properties of Polymer Matrix Composite Materials”. Table 2 shows the experimental findings. Untreated SiC in 1 vol. % doesn’t lead to any improvement in tensile properties of Kevlar/vinyl ester composites. The SiC nanoparticles, due to their high surface energy coupled with the high surface area, attract the hydrophilic polar portion of vinyl ester molecules resulting in the mobility reduction of polymer molecules and hence an increase in resin viscosity [14]. The increased viscosity promotes void formation and impairs both the wetting and infiltration of the Kevlar fabrics, which in conjunction with the loosely assembled SiC nanoparticle agglomerates and poor particle-matrix bonding cause the lack of reinforcing effect with untreated SiC. However, a 19% increase in tensile strength was observed when the fiber-nanocomposite panel was fabricated using MPS. The addition of MPS enhances the particle-matrix interfacial bonding, improves the SiC dispersion, and causes a reduction in resin viscosity attributed to its surface-active properties [2], which contributes to the observed improvement in tensile strength.

Mixing condition	Tensile strength (MPa)					Mean	S.D.
	X ₁	X ₂	X ₃	X ₄	X ₅		
0% SiC Remarks	340	> 347 at clamp	349	> 352 didn't break	329	343	9
1 vol. % SiC without dispersant	> 246 at clamp	> 272 at clamp	> 316 didn't break	340 didn't break	343	341	2
1 vol. % SiC with MPS - In situ	407	> 385 didn't break	400	415	412	408	7

TABLE 2 Summary table of panels' tensile properties.

Remarks: "at clamp" – fabrics broke at clamping area; "didn't break" – panel specimen slipped at clamping area.

4. CONCLUSIONS

Nanotechnology has opened a new chapter in composites manufacturing by the addition of nanoparticles to conventional fiber-reinforced composites. Because the SiC nanoparticles are small (~30nm) and their surface hydrophilic, as well as the high surface energy of SiC acting as the driving force for agglomeration, their dispersion is difficult in a vinyl ester (oleophilic system) resin. It is observed that optimum treatment of MPS, as shown by a better state of dispersion of SiC particles in vinyl ester resin, correlates well with the performance of composites as measured by flexural and tensile strength. The results suggest that a synergistic interaction between the vinyl ester resin, SiC nanoparticles, and Kevlar fibers may have contributed to the improved mechanical properties observed with low SiC particle loading.

5. ACKNOWLEDGMENT

We would like to thank the AFOSR and the U.S. Army for financial support through AFOSR Grant F49620-02-1-0414, Dr. John W. Goodman for his advice and to Alessandro Dini for TEM micrographs.

6. REFERENCES

1. Roco, M.C. (1999) "Nanoparticles and nanotechnology research", *Journal of Nanoparticle Research*, 1(1): 1-6.
2. Plueddemann, E.P. (1991) *Silane Coupling Agents*. Plenum Press.
3. Philipse, A.P. and Vrij, A. (1989) "Preparation and properties of nonaqueous model dispersions of chemically modified, charged silica spheres", *Journal of Colloid and Interface Science*, 128(1): 121-136.

4. Ishida, H. and Koenig, J.L. (1980) "A Fourier-transform infrared spectroscopic study of the hydrolytic stability of silane coupling agents on E-glass fibres", *Journal of Polymer Science, Polymer Physics Edition*, 18(9): 1931-1933.
5. Gutowski, T.G. (1997) *Advanced Composites Manufacturing*. Wiley.
6. Preiss, H., Berger, L.-M., and Braun, M. (1995) "Formation of black glasses and silicon carbide from binary carbonaceous/silica hydrogels", *Carbon*, 33(12): 1739-1746.
7. Jancar, J. (1999) *Mineral Fillers in Thermoplastics I: Raw Materials and Processing*. Advances in Polymer Science, Vol. 139. Springer Verlag.
8. Das, D., Farjas, J., Roura, P., Viera, G., and Bertran, E. (2001) "Thermal oxidation of polymer-like amorphous $\text{Si}_x\text{C}_y\text{H}_w\text{O}_z$ nanoparticles", *Diamond and Related Materials*, 10(3-7): 1295-1299.
9. Brewer, C.M., Bujalski, D.R., Parent, V.E., Su, K., and Zank, G.A. (1999) "Insights into the oxidation chemistry of SiOC ceramics derived from silsesquioxanes", *Journal of Sol-Gel Science & Technology*, 14(1): 49-68.
10. Sun, Y. and Miyasato, T. (1998) "Infrared absorption properties of nanocrystalline cubic SiC films", *Japanese Journal of Applied Physics Part 1-Regular Papers Short Notes & Review Papers*, 37(10): 5485-5489.
11. Kamiya, H., Mitsui, M., Takano, H., and Miyazawa, S. (2000) "Influence of particle diameter on surface silanol structure, hydration forces, and aggregation behavior of alkoxide-derived silica particles", *Journal of the American Ceramic Society*, 83(2): 287-293.
12. Silverstein, R.M. and Webster, F.X. (1998) *Spectrometric Identification of Organic Compounds*. Wiley. 6th ed.
13. Wei, D., Dave, R., and Pfeffer, R. (2002) "Mixing and characterization of nanosized powders: an assessment of different techniques", *Journal of Nanoparticle Research*, 4(1-2): 21-41.
14. Lee, B.L., Roslund, A., Rude, T.J., Castren, G.C., and Takacs, E.J. (2001) "Processing of macroscopic fiber composites with dispersion of nanoparticles in resin matrix", *221st American Chemical Society National Meeting, Symposium on Defense Applications of Nanomaterials*.